論文の内容の要旨

論文題目

Structure and behaviour of pure and salty ice VII
from *in-situ* neutron diffraction techniques
with development of high-pressure cells

(高圧セル開発とその場中性子回折による
純粋および塩を含む氷 VII 相の構造と挙動)

氏名　山下 恵史朗

Water is a ubiquitous material and also one of the simplest molecules. In spite of its simplicity as a molecule, water has a structural variety in condensed phases. Water molecules are regarded as a tetrahedrally building unit in ice structures. Ice VII is a crystalline phase of water and stable above 2 GPa at room temperature. Its structure can be expressed by a highly symmetric cubic model called the "single-site" model (Figure 1). The orientations of water molecules are disordered in ice VII, but they become ordered in ice VIII at low temperature retaining the topology of the hydrogen bonding network. Ice VII exhibits unique behaviours such as cross-over of proton dynamics at 10 GPa [1] and symmetrisation of hydrogen bonds towards ice X at 60 GPa [2]. Moreover, ice VII is reported to structurally incorporate ionic species in contrast to ordinary ice I [3–5]. Neutron diffraction is a strong technique to investigate the structures for their sensitivity to hydrogen (deuterium). In this thesis, I investigated the structures and thermodynamic behaviours of pure and salty ice VII from neutron diffraction experiments under high pressure.

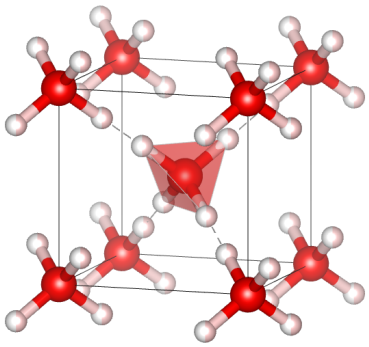

Figure 1: Single-site model of ice VII with tetrahedron describing coordination geometry of water molecule.

Chapter 2 describes developments of diamond anvil cells (DACs) for single-crystal neutron diffraction with their feasibility test on diffraction measurements. Single-crystal diffraction is the basis of diffraction techniques because it provides three-dimensional information, whereas powder diffraction inevitably reduces structural information into one dimension as a result of orientational averages of crystallites. However, single-crystal diffraction is still challenging for high-pressure experiments because neutron beams are blocked by bulky high-pressure vessels. I overcame this limitation by isolating the sample from a massive loading frame using special materials: nano-polycrystalline diamond (NPD) for anvils and Zr-based bulk metallic glass (BMG) for a cylinder [6] (Figure 2). Both NPD and Zr-BMG are highly neutron transparent so that neutron beams can travel through the DAC with sufficient intensity from/to arbitrary directions. Moreover, these materials do not produce serious parasitic diffractions. Such extra diffraction from conventional materials such as alloys and single-crystalline diamonds are harmful to distinguish the signals from the sample.

The developed DAC was confirmed to stably generate 4.5 GPa, sufficient pressure for this study. For

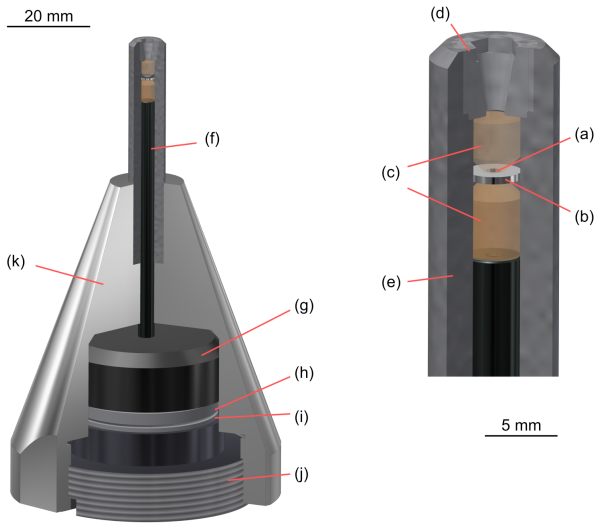

Figure 2: Schematic image of the developed DAC; (a) sample, (b) gasket, (c) anvils, (d) back nut, (e) cylinder, (f) piston tube, (g) piston, (h) bearing, (i) spacer, (j) back screw, and (k) body.

comparison with the conventional sample mounting, diffraction patterns were collected for NaCl and NH_4Cl at the D9 beamline of the Institut Laue-Langevin (ILL, France) and at the BL18 (SENJU) beamline of the Material and Life Science Experimental Facility (MLF) at J-PARC (Ibaraki, Japan), respectively. Both experiments resulted in plausible structure refinements with R-factors better than 10% with tiny crystals smaller than 0.1 mm^3. High-pressure diffraction measurements were also conducted for pure ice VI at *ca.* 1 GPa.

Chapter 3 describes detailed structure analyses of pure ice VII by the combination of single-crystal and powder neutron diffraction. The single-site model is adopted in many studies because of its simplicity and reproducibility of diffraction patterns. However, it gives an unrealistic molecular geometry in the structure refinement such as an unlikely short O-D covalent bond length of 0.89 Å quite shorter than that in ice VIII (0.97 Å) [7]. This is because the structure model, averaged in time and space, does not match the intrinsic atomic positions. Then structure models with multiple displaced sites have been proposed to describe the structure of ice VII with plausible molecular geometry [7, 8]. However, no unambiguous structure refinements have been achieved so far due to the small displacements to determine experimentally. In this study, neutron diffraction measurements were conducted on single crystals and powder samples using the developed DAC at the D9 and MITO system [9] at the BL11 (PLANET) beamline, MLF, J-PARC, respectively. Deuterated samples were used to avoid incoherent scattering.

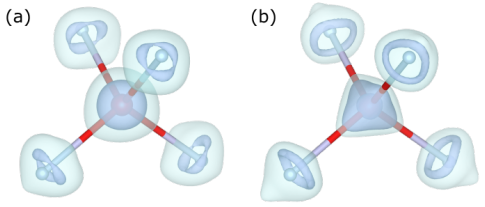

Figure 3: Atomic distribution in ice VII at 298 K and 2.2 GPa derived from (a) single-crystal and (b) powder diffraction data. The oxygen and deuterium are illustrated by the single-site model with O-D = 0.97 Å.

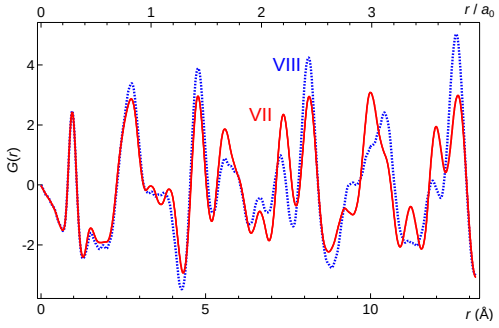

Figure 4: Pair distribution functions $G(r)$ of ice VII (red solid line) and VIII (blue dotted line) obtained at 274 K and 2.2 GPa. The top abscissa is normalised interatomic distance by the length of an edge of the unit-cell of ice VII a_0 = 3.346 632 Å derived in the Rietveld analysis.

Three-dimensional atomic distributions were obtained by applying a maximum entropy method (MEM) to both diffraction data at 2.2 GPa and 298 K (Figure 3). The derived density distributions revealed unexpected ring-like distributions of deuterium around the average O-O axis as well as oxygen displacement along ⟨111⟩ directions. Those could not be clarified in previous diffraction studies.

The interatomic structures of ice VII and VIII were derived by a total scattering analysis of the powder diffraction data at 274 K and 2.2 GPa (Figure 4). Individual peak fitting gave the O-D distance of 0.9662(5) Å in ice VII comparable to that in ice VIII as expected. Despite the similarity of the pair distribution function (PDF), $G(r)$, of ice VII and VIII at the short distances, they differed at longer distances than the size of the unit cell of ice VII (≈ 3.3 Å). These findings indicate that molecular behaviours are actually identical between ice VII and VIII, but their intermolecular structure is distinct between them. The apparently short O-D distances in ice VII obtained by conventional structure analyses are caused by spatial and time averaging of the various molecular configurations in the disordered structure of ice VII.

Chapter 4 describes the behaviours of salty ice VII in its excess volumes and hydrogen disordering. Ice VII is known to structurally incorporate salt such as NaCl, LiCl, $MgCl_2$ [3–5], *etc.* in contrast to ordinary ice I_h. Salt-incorporated ice VII can be prepared in two ways. A path via amorphisation at low temperature before compression is the way for salty VII with high salinity up to 15 mol% [10]. The obtained salty ice VII has drastic volume expansion and disturbance of hydrogen ordering at low temperature. Compression at room temperature from liquid phase gives one with lower salinity than 2 mol% [3, 5]. There is a gap between these studies which cannot be explained in a simple doping description. I investigated the volume change and hydrogen ordering of salty ice VII by sequential measurements of neutron powder diffraction using the MITO system at the BL11 (PLANET).

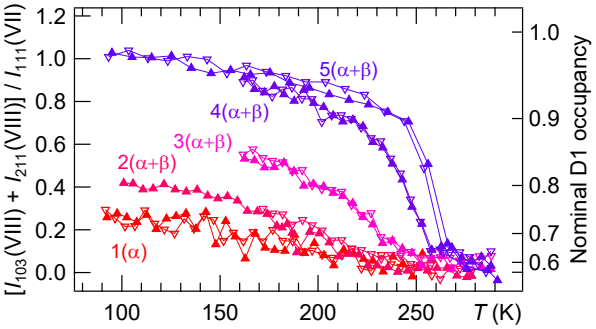

Figure 5: Temperature dependencies of hydrogen ordering features in path A. Summed diffraction intensities corresponding to 103 and 211 diffraction of ice VIII are normalised by that of 202 peak of ice VIII (111 of ice VII) at the highest temperature in each cycle. Downward open and upward filled triangles indicate cooling and heating procedures, respectively. The numbering of each plot correspond to annealing steps at 1) 265 K, 2) 285 K, 3) 315 K, 4) 340 K, and 5) 370 K. The right ordinate corresponds to nominal D1 occupancy calculated from a structure model of partially ordered ice VIII with cubic symmetry.

Salty ice VII was obtained starting from solutions of $MgCl_2$:D_2O = 1:25 (in molar) via saline amorphous at low temperature in two runs. A salty ice VII crystallised during heating at *ca.* 4 GPa in path A with the excess volumes over 5% compared to pure ice [11]. This large volume expansion was also observed in the other run. α-VII did not show features of hydrogen ordering (Figure 5) like the reported case of LiCl [4]. After further annealing at higher temperatures, the peaks of ice VII was broadened and split into two types of ice VII apparently. The other ice VII (hereafter β-VII) had smaller excess volumes and showed the increase of the hydrogen ordering features according to annealing. α-VII disappeared after further annealing while β-VII remained with volume decrease into 0%. Thus β-VII would be described by a simple doping model like as discussed in the salty ices obtained at ambient pressure compression [5]. The features of α-VII had a gap from β-VII suggest α-VII would be somewhat metastable with non-negligible potential minima. Although

α-VII is energetically unfavoured at higher temperatures, it would be not simply a kinetically-trapped state like β-VII. It is not clear what is the main factor of their differences, but the structural difference is considered to be the major factor considering the fact that diffraction peaks of salt hydrates became obvious after α-VII almost disappeared.

In conclusion, I clarified the detailed structure of pure ice VII by single-crystal neutron diffraction using the newly-developed DAC combined with powder diffraction. Ice VII has a distinct intermolecular structure from its ordered counterpart, ice VIII, but the molecular geometry is identical as expected empirically. The atomic distribution derived by the MEM analysis highlighted the insufficiency of the discrete structure models to describe the disordered structure of ice VII. From *in-situ* powder neutron diffraction, I proposed two types of salty ice VII crystallised from saline amorphous depending on further annealing. They are considered to qualitatively explain the previously reported salty ice VIIs. Moreover, crystallisation from amorphous phases is a long-standing issue in which kinetic factors compensate for thermodynamic stability at low temperatures. As supposed for pure ices (*e.g.* [12]), the crystalline phases and amorphous would have structural similarity. Further investigations with distinguishing α- and β-VII will be a new window for the comprehensive understanding of the ambiguous amorphous and salt-incorporated ice VII.

References

1. Yamane, R. *et al. Phys. Rev. B* **104,** 214304 (2021).
2. Lee, C. *et al. Phys. Rev. Lett.* **69,** 462–465 (1992).
3. Frank, M. R. *et al. Phys. Earth Planet. Inter.* **155,** 152–162 (2006).
4. Klotz, S. *et al. Nat. Mater.* **8,** 405–409 (2009).
5. Watanabe, M. *et al. Jpn. J. Appl. Phys.* **56,** 05FB03 (2017).
6. Yamashita, K. *et al. High Press. Res.* **40,** 88–95 (2020).
7. Kuhs, W. F. *et al. J. Chem. Phys.* **81,** 3612–3623 (1984).
8. Nelmes, R. J. *et al. Phys. Rev. Lett.* **81,** 2719–2722 (1998).
9. Komatsu, K. *et al. High Press. Res.* **33,** 208–213 (2013).
10. Klotz, S. *et al. Sci. Rep.* **6,** 32040 (2016).
11. Klotz, S. *et al. Phys. Rev. B* **95,** 174111 (2017).
12. Shephard, J. J. *et al. J. Phys. Chem. Lett.* **8,** 1645–1650 (2017).